High piezoelectric and mechanical performances in multiferroic (1-*x*-*y*)$PbTiO_3$-*x*$Bi(Ni_{1/2}Ti_{1/2})O_3$-*y*$BiScO_3$**

By *Penghao Hu, Jun Chen, Ziyou Yu, Lili Zhou, Jinxia Deng, and Xianran Xing*[*]

Electronic supplementary information

Experimental details

The modified solid state reaction method was adopted to prepare (1-*x*-*y*)$PbTiO_3$-*x*$Bi(Ni_{1/2}Ti_{1/2})O_3$-*y*$BiScO_3$ using analytic reagent grade raw materials, PbO, Bi_2O_3, NiO, Sc_2O_3 and TiO_2 (anatase). Stoichiometric starting reagents were ball-milled in ethanol for 24 h. Dried powders were pressed into pellets of 11 mm in diameter and 2-3 mm in thickness and then calcined at 800 ^oC for 5 h. Part of calcined powders were pressed into pellets in the same size, and sintered at 1100~1150 ^oC for 5 h covered with the remaining powders to compensate the evaporation loss of PbO and Bi_2O_3. After removing the surface layers of the sintered pellets carefully, the pellets were grinded into powders, and then annealed at 800 ^oC for 1 h to remove the mechanical strain introduced during the sintering and grinding processes.

Phase identification and structural characterization were conducted from X-ray diffraction (XRD) technique on a 21 kW extra-power powder diffractometers (model M21XVHF22, Mac Science, Yokohama, Japan). The lattice parameters were calculated by *PowderX* and *TREOR* software. The ferroelectric polarization-field and the strain-field butterfly loops were measured for specimens with diameter of ~10 mm and thickness of ~0.4 mm by ferroelectric tester (Model aixACCT, TF Analyzer 1000).

[*] Corresponding author Electronic mail: xing@ustb.edu.cn. Tel.: +86-10-62334200. Fax: +86-10-62332525.

The piezoelectric property of the poled ceramics with an Ag electrode was measured using a quasi-static d_{33} meter (China Academy of Acoustics, ZJ-3). Poling was performed at 120 ^{o}C under a saturated dc filed of about 5 kV·mm^{-1}, applied for 5 min. The magnetic loops were performed using a Quantum Design physical property measurement instrument (Magnetic Property Measurement System-5). Micrographs of the ceramics were characterized on field-emission scanning electron microscopy (FE-SEM, LEO1530). The apparent thermal expansion coefficients and the thermal cycles curves on the ceramics were determined using a Thermal mechanical analyzer (Setaram Setsys Evolution) with pellet samples (diameter 10 mm, thickness ~2 mm) at a heating and cooling speed 5 ^{o}C·min^{-1}. Vickers indentation hardness of the materials was carried on a Digital Microhardness tester (MH-6, Shanghai) with different loads and 15 s of dwell time.

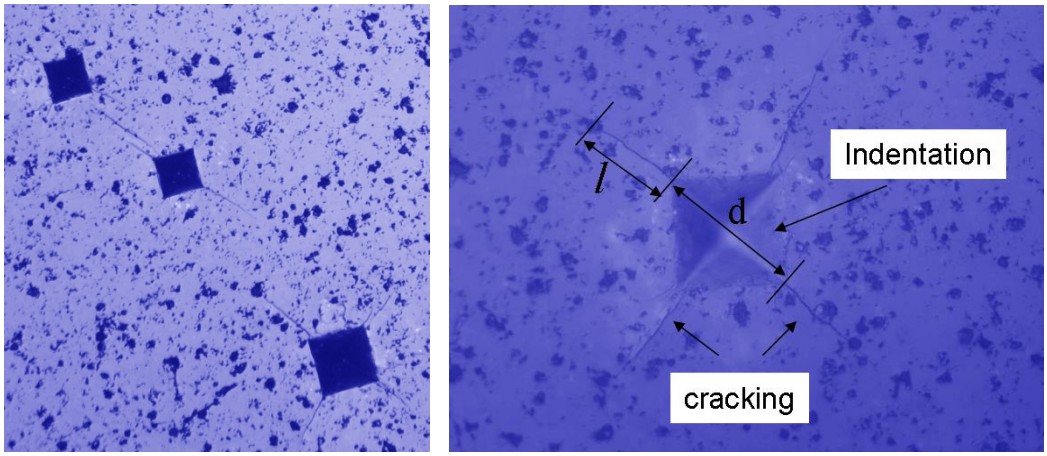

Figure S1. A typical photograph of indentation in the Vickers indentation hardness measurement.

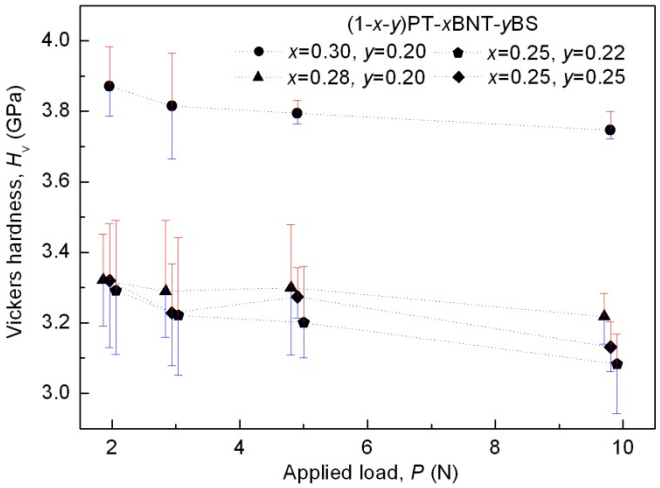

Figure S2. Vickers indentation hardness of (1-*x*-*y*)$PbTiO_3$-*x*$Bi(Ni_{1/2}Ti_{1/2})O_3$-*y*$BiScO_3$ ceramics under different loads.

The Vickers indentation hardness (H_v) of the PT-BNT-BS ceramics were characterized by a digital microhardness tester and the fracture toughness (K_{IC}) were calculated by the reported equation[*]:

$$K_{IC} = \frac{0.0624P}{dl^{1/2}}$$

where *d* is diagonal length of the indentation, *l* is the crack's vertical length measured from the tip of indentation. The *d* and *l* were measured directly from the photographs (See Fig. S1). Generally, the longest crack was measured for the *l* magnitude. The K_{IC} obtained under different loads were counted for the average values (See Table 2 in the manuscript).

[*] Zhang, H.; Su, Y. J.; Qiao, L. J.; Chu, W. Y.; Wang, D.; Li, Y. X. *J. Elec. Mat.* **2008**, *37*, 368.

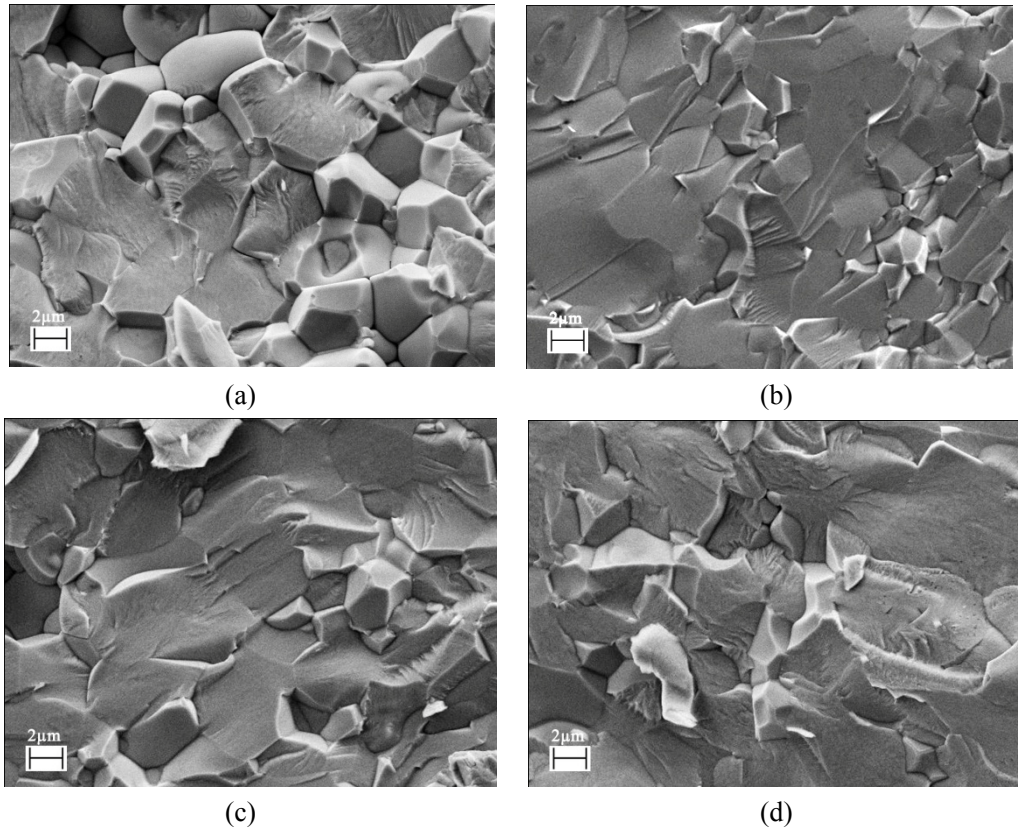

(a) (b)

(c) (d)

Figure S3. SEM fracture micrographs of the (1-*x*-*y*)$PbTiO_3$-*x*$Bi(Ni_{1/2}Ti_{1/2})O_3$-*y*$BiScO_3$ ceramics, solubility (a) $x = 0.30$, $y = 0.20$ (b) $x = 0.28$, $y = 0.20$, respectively. The graphs (c) and (d) are the fracture morphology of the corresponding ceramics after 2 heating and cooling cycles from room temperature to 800 ^{o}C.

The fracture morphology represent transcrystalline rupture which reveals the ceramics are well sintered and compact with high fracture toughness. The morphology in graphs (c) and (d) are similar to that of the corresponding ceramics in graphs (a) and (b) which demonstrates that the ceramics after 2 heating and cooling cycles well retained their crystal structure and density, they represent high thermal stability.